

Interface solar evaporator synergistic phase change energy storage for all-day steam generation

Le Geng, Lele Li, He Zhang, Minjuan Zhong, Peng Mu*, and Jian Li*

Key Laboratory of Eco-functional Polymer Materials of the Ministry of Education, College of Chemistry and Chemical Engineering, Northwest Normal University, Lanzhou 730070, P. R. China.

* Corresponding author: pengmu2019@nwnu.edu.cn (P. Mu); jianli83@126.com (J. Li).

Characterization

The microstructure and morphology of nylon thread, PNT, octadecane, PPy, Cppy, PPy-O and Cppy-O were characterized by a field emission scanning electron microscopy (FE-SEM, Ultra Plus, Zeiss) and transmission electron microscope (JEM2100). The chemical composition and function groups were analyzed by FTIR spectra (Bio-Rad FTS-165). The UV-Vis-NIR absorption was conducted at UV-Vis-NIR spectrometer Lambda 750 from 200~2500 nm equipped with an integrated sphere. Differential scanning calorimetry (DSC) analysis were collectively conducted at a heating and cooling rate of 5 K min⁻¹ in a nitrogen atmosphere (METTLER TOLEDO). The contact angles of nylon thread and PPy-nylon thread were measured by contact angle apparatus (SL200KB).

Solar steam generation test

The solar steam generation experiments were conducted at a lab-made, online, real-time measurement system which consists of a light simulation system and a detection system. The light simulation system including a solar light simulator (Xenon arc lamp, CEL-S500, Ceaulight) with a solar filter (AM 1.5, Ceaulight) and a light intensity was

measured by a full spectrum optical power meter (CEL-NP2000-2, Beijing Education Au-light Co., Ltd.) The detection system including a test chamber is an open cylinder with 80 mm in height 27 mm in diameter, an analytical balance (FA 2004), a computer to record the time-dependent mass change of water due to the steam generation and an infrared camera (Testo 869, Germany). During the evaporation process, three evaporators were placed in expandable polyethylene foam with holes at the bottom, which acts as a thermal isolation layer and support substrate that allows the entire device to float on water surface. During all tests, the room temperature was maintained at 23–25 °C and the humidity was ranged from 30 %-35 %.

Evaporation test details

(Salt resistance performance) The Cavity and Cppy-O evaporators were soaked directly in different concentration NaCl solution (3.5%, 5%, 10%, 15%, and 20%), and measured under light simulation system to evaluate the salt resistance performance.

Calculation of the solar-to-vapor efficiency

$$\eta = \frac{mh_{LV}}{C_{opt}q_i}$$

where m is the evaporation rate ($\text{kg}\cdot\text{m}^{-2}\cdot\text{h}^{-1}$) as mentioned without subtracting the water evaporation in dark field, as reported by Gan et al [1], C_{opt} refers to the optical concentration on the absorber surface, q_i is the nominal direct solar irradiation $1 \text{ kW}\cdot\text{m}^{-2}$, h_{LV} is total enthalpy of liquid-vapor phase change (including sensible heat and phase-change enthalpy) vaporization enthalpy of the water in Cppy-O evaporator, which can be calculated as:

$$h_{LV} = C\Delta T + h_{vap}$$

where h_{vap} is latent heat of phase change, C is specific heat capacity of water ($4.2 \text{ kJ}\cdot\text{kg}^{-1}\cdot\text{K}^{-1}$), and ΔT denotes the temperature increase of the water. Table S1 shows the latent heat of evaporation of water at various temperatures [2]. Due to the evaporation enthalpy of water folled in polymer will signigicantly change, the evaporation enthalpy of water in sample was corrected via a calibration test [3-5]. Pure water and Cppy-O evaporator with same superficial area were synchronously located in a closed desiccator with supersaturated potassium carbonate solution to maintain the relative humidity about 45% and the temperature at 25 °C and ambient air pressure[4].

$$h_{\text{vap}} m_{\text{PPy1-P}} = h_{\text{LV},T_s} m_{\text{water}}$$

The result of real evaporation enthalpy is shown in Table S2. Therefore, the solar-vapor efficiency can be estimated to be

$$\eta_{\text{water}} = \frac{m h_{\text{LV}}}{C_{\text{opt}} q_i} = \frac{0.38 \times (2409 + 0.001 \times 4.2(30.9 - 24))}{1 \times 3600} = 25.4\%$$

$$\eta_{\text{Cavity}} = \frac{m h_{\text{LV}}}{C_{\text{opt}} q_i} = \frac{2.24 \times (1273.8 + 0.001 \times 4.2(43.1 - 24))}{1 \times 3600} = 79.2\%$$

Sample	Mass change (g)	Theoretical latent heat ($\text{J}\cdot\text{g}^{-1}$)	Real vaporization enthalpy ($\text{J}\cdot\text{g}^{-1}$)
Pure water	1.2475	2409	2409
Cppy-O	2.3592	2409	1273.8

$$\eta_{\text{OCC}} = \frac{m h_{\text{LV}}}{C_{\text{opt}} q_i} = \frac{2.26 \times (1273.8 + 0.001 \times 4.2(42.4 - 24))}{1 \times 3600} = 79.9\%$$

$$\eta_{\text{Cppy-O}} = \frac{m h_{\text{LV}}}{C_{\text{opt}} q_i} = \frac{2.62 \times (1273.8 + 0.001 \times 4.2(41.7 - 24))}{1 \times 3600} = 92.7\%$$

Table S1. The result of evaporation enthalpy by calibration test.

Table S2. The latent heat of evaporation of water at various temperatures

Temperature (°C)	Kelvin temperature scale (K)	Latent heat (J·g ⁻¹)
25	298.15	2442.4
26	299.15	2440.4
27	300.15	2438.3
28	301.15	2436.2
29	302.15	2434.2
30	303.15	2432.1
31	304.15	2430.1
32	305.15	2428.1
33	306.15	2426.1
34	307.15	2424.2
35	308.15	2422.2
36	309.15	2420.3
37	310.15	2418.4
38	311.15	2416.5
39	312.15	2414.6
40	313.15	2412.7
41	314.15	2410.8
42	315.15	2409.0
43	316.15	2407.1

Calculation of the light absorption ability

The light absorptivity of the membrane can be calculated by using the equation:

where A is the absorbance, R is the reflectance, and T is the transmittance.

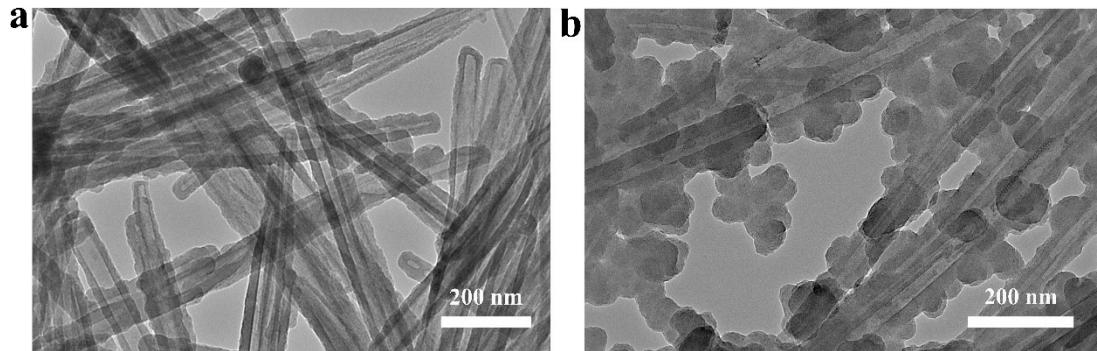


Figure S1 The TEM images of (a) Cppy aerogel, (b) Cppy-O phase change composite material.

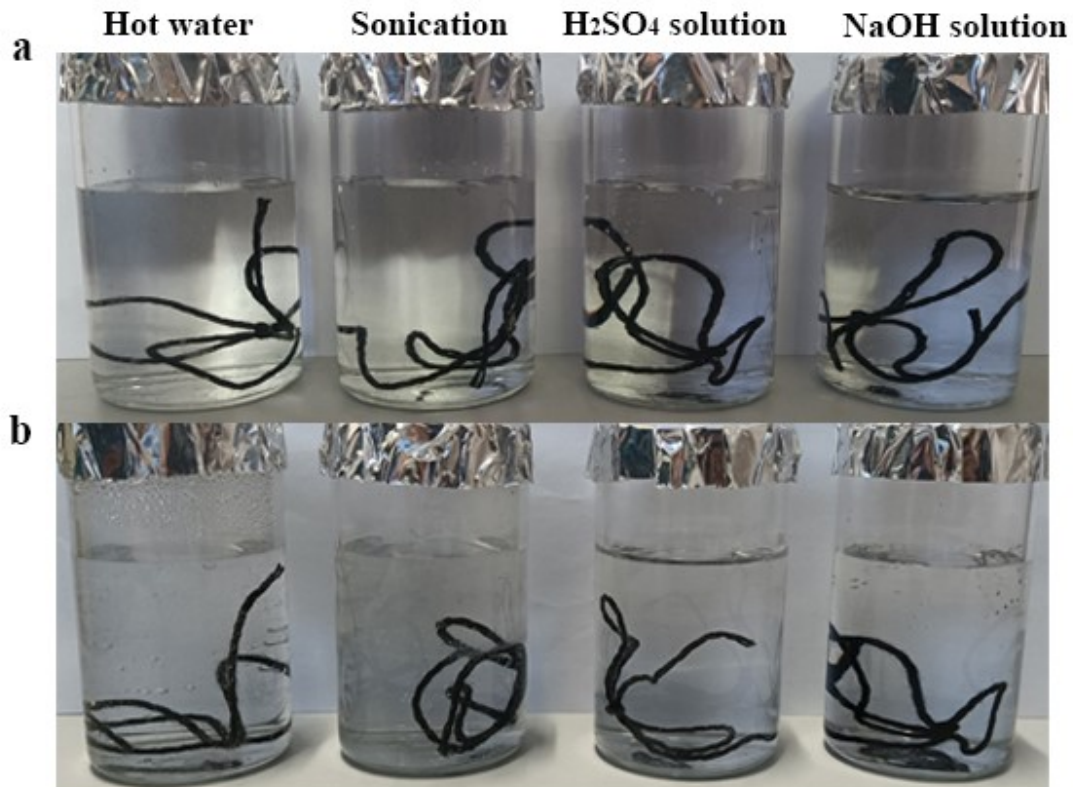


Figure S2 The optical photographs of PNT before and after hot water, sonication, 1M H_2SO_4 , and 1M NaOH treatments for 3 hours.

- [1] Z. Liu, H. Song, D. Ji, C. Li, A. Cheney, Y. Liu, N. Zhang, X. Zeng, B. Chen, J. Gao, Y. Li, X. Liu, D. Aga, S. Jiang, Z. Yu, Q. Gan, Extremely Cost-Effective and Efficient Solar Vapor Generation under Nonconcentrated Illumination Using Thermally Isolated Black Paper, *Global Chall* 1 (2017) 1600003.
- [2] S. Chen, Z. Sun, W. Xiang, C. Shen, Z. Wang, X. Jia, J. Sun, C.-J. Liu, Plasmonic wooden flower for highly efficient solar vapor generation, *Nano Energy* 76 (2020) 104998.
- [3] Y. Guo, H. Lu, F. Zhao, X. Zhou, W. Shi, G. Yu, Biomass-Derived Hybrid Hydrogel Evaporators for

Cost-Effective Solar Water Purification, *Adv. Mater.* 32 (2020) 1907061-1907069.

[4] F. Zhao, X. Zhou, Y. Shi, X. Qian, M. Alexander, X. Zhao, S. Mendez, R. Yang, L. Qu, G. Yu, Highly efficient solar vapour generation via hierarchically nanostructured gels, *Nat. Nanotechnol.* 13 (2018) 489-495.

[5] Q. Lu, W. Shi, H. Yang, X. Wang, Nanoconfined Water-Molecule Channels for High-Yield Solar Vapor Generation under Weaker Sunlight, *Adv. Mater.* 32 (2020) 2001544-2001551.